Arabian Journal of Geosciences (2021) 14: 2049
https://doi.org/10.1007/s12517-021-08435-y

ORIGINAL PAPER

Layout design specifications of hard-rock TBM cutterheads at maximum cutter penetration and TBM advance

Ebrahim Farrokh[1]

Received: 24 August 2020 / Accepted: 9 September 2021 / Published online: 22 September 2021

Abstract

Evaluation of optimum rock cutting performance is very important, especially at the phase of the design of a tunneling machine. In this regard, existing theoretical, laboratory, numerical, or empirical methods focus only on the optimum ratio of cutter spacing over penetration, and they need further enhancements to include various design aspects of the TBM cutterhead with respect to cut and cutter geometry parameters as well as its major layout design characteristics. Field data analysis is regarded as the most accurate and reliable method in the industry as it covers various geological conditions (which is not as easy in the laboratory or numerical simulations), and it provides new practical formulas to evaluate TBM performance. To investigate the influence of various parameters on the cutter penetration and to provide a basic guideline to optimize field cutter spacing and cutterhead layout design, an extensive field database is compiled. With the use of this database, the effects of rock type and uniaxial compressive strength on cutter penetration are investigated in various categories of cutter spacing. Major layout designs of the cutterheads utilized in various rock types and different categories of tunnel sizes are investigated for projects with relatively high performance. The results of the conducted analyses show that the maximum cutter penetration in uniaxial compressive strength values below 50 and above 150 MPa is achieved close to 90 and below 80 mm, respectively. The results of the study on the layout design characteristics of the cutterhead indicate that the evenly distributed scheme is more used with success even in softer rocks (when the rock mass condition is good). In softer rocks, the extension of the openings has to be well over 50% of the cutterhead radius to maximize its performance. In this regard, some empirical formulas are generated through statistical analysis of the data from around 300 tunnel projects to evaluate both optimum cutter spacing and optimum ratio of cutter spacing over penetration. New formulas are also provided to evaluate cutterhead thrust, torque, RPM, and power. In the end, based on the discussed issues, to optimize cutter penetration and TBM cutterhead overall performance, some procedural steps are offered.

Keywords TBM · Cutterhead · Cutter spacing · Layout design · Optimization

Introduction

In recent years, tunnel boring machines (TBMs) have been widely used in various projects around the world. As the competition among various contractors is increasing, the project engineers have to always search for optimization processes to increase projects' performance. In this regard, for the TBM, specific energy was one of the main parameters that has been extensively studied for the optimization. The literature shows various laboratory tests using the linear cutting machine (e.g., Abu Bakar et al. 2014; Cho et al. 2013; Eskikaya et al. 2005; Gertsch et al. 2007; Ozdemir et al. 1978; Rostami 1993, 1997; Roxborough and Phillips 1975; Sanio 1985; Snowdon et al. 1982; Tuncdemir et al. 2008; Choi et al. 2014; Ma et al. 2016a, 2016b; Pan et al. 2018a, Gong et al. 2015, 2016a, 2016b, 2016c) and the rotary cutting machine (Farrokh et al. 2015; Qi et al. 2016; Gong et al. 2016b) have been utilized to investigate the relationships between specific energy and cut and cutter geometry characteristics. Besides, numerical simulations have been also widely used to study the issues of specific energy and cutter forces (Innaurato et al. 2007; Liu et al. 2002; Ma et al. 2011; Gong et al. 2006a, 2006b; Labra et al. 2016; Liu et al. 2016a, 2016b, 2016c; Park et al. 2018).

Responsible editor: Murat Karakus

✉ Ebrahim Farrokh
e.farrokh@aut.ac.ir

[1] Amirkabir University of Technology (Tehran Polytechnic), Tehran, Iran

These studies indicate, in order to reach an optimum excavation, the ratio of cutter spacing to penetration (*S/p*) shall be varied to reach minimum specific energy (*SE*). At this *SE*, the rolling force required to generate a unit volume of the excavated rock is comparably lower. One note is that in practice, rolling force is much lower than the normal force (less than 20% of the normal force as noted by Pan et al. (2018a, 2018b, 2019), Thyagarajan (2018), Tumac and Balci (2015),

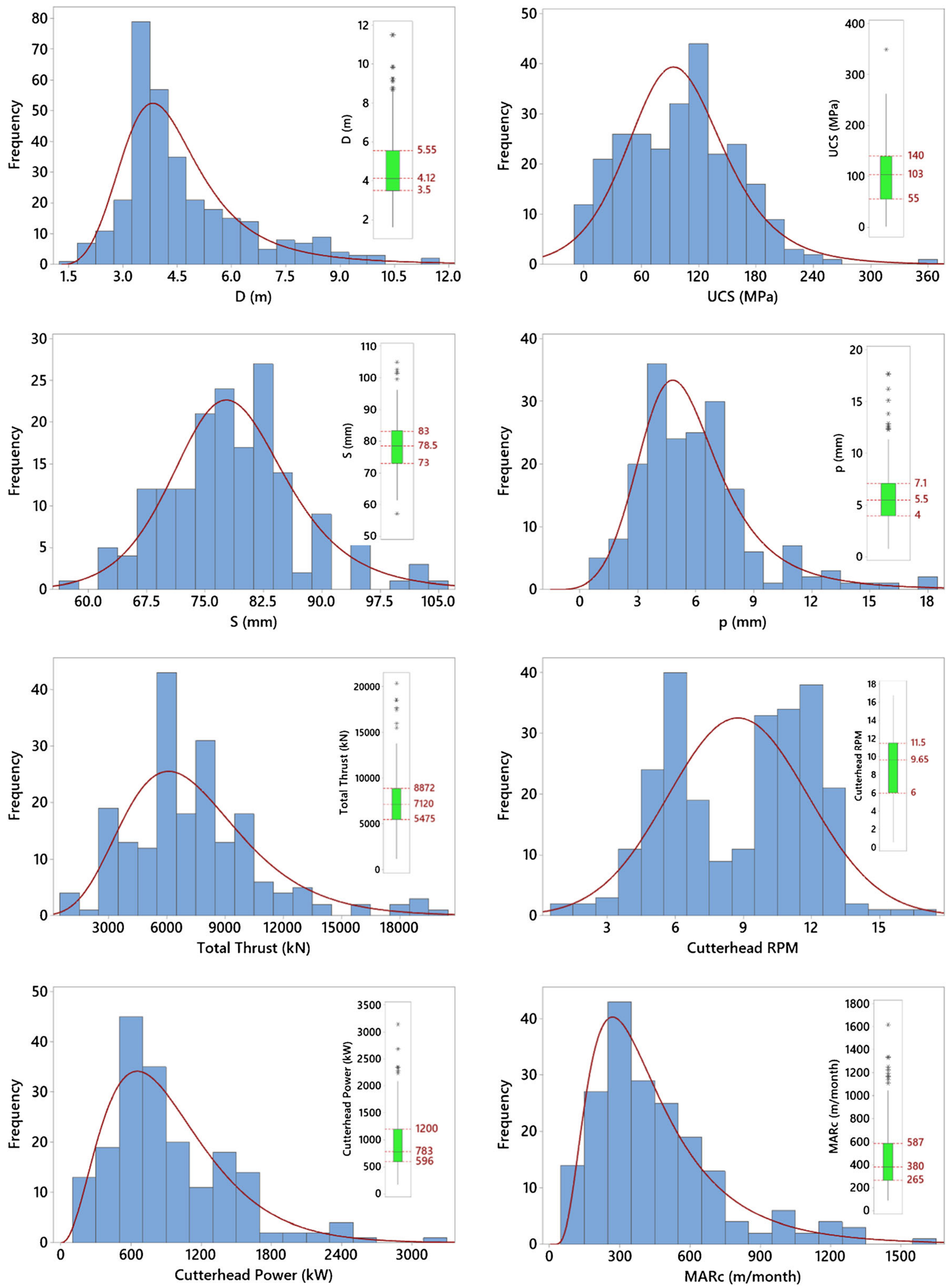

Fig. 1. The distribution of the main parameters included in the database

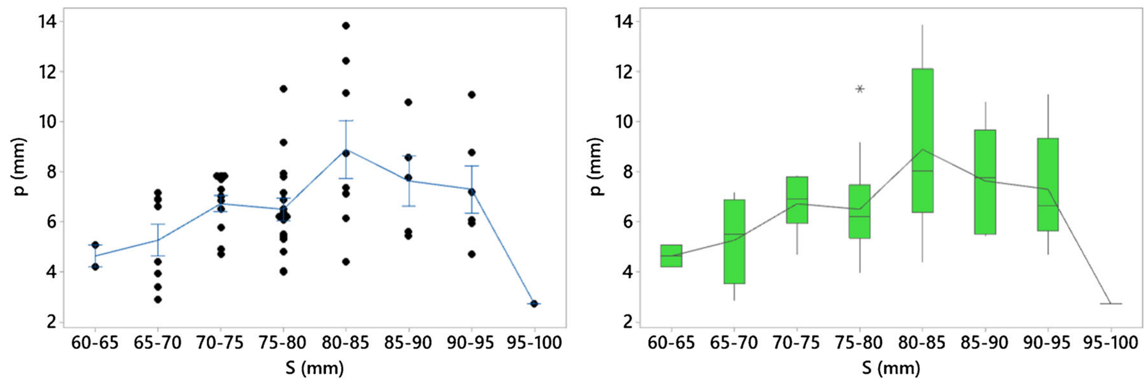

Fig. 2. Correlation between cutter spacing and cutter penetration for sedimentary rocks

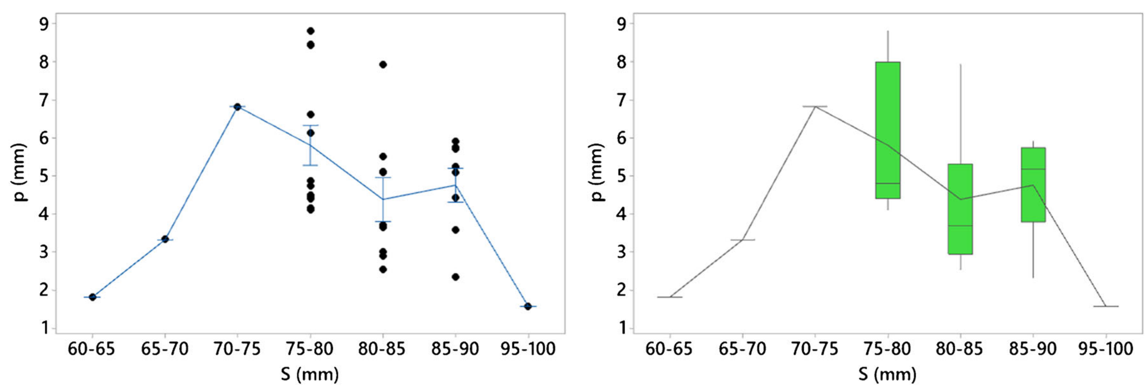

Fig. 3. Correlation between cutter spacing and cutter penetration for metamorphic rocks

Abu Bakar et al. (2014), Gertsch et al. (2007), Cho et al. (2010), and Balci (2009). This is because the normal force firstly causes the radial cracks to develop beneath the cutters. Then the rolling force dislodges the fractured rock from its place. The energy to create the radial cracks is much higher than the energy to dislodge the fractured rock. This leads to a higher normal force.

For this reason, the rolling force value is not a major concern in performance optimization as long as its value falls within its permissible limit defined by the maximum cutterhead torque. As an example, in an 8.75-m hard-rock TBM project, the rock type was granite and granodiorite with 100–250 MPa uniaxial compressive strength. The normal force on the 17-inch cutters reached around 220 kN which is close to the maximum cutter load capacity; however, the rolling force reached only around 10 kN with a total cutterhead torque of 1250 kNm. This is around 10% of the maximum installed cutterhead torque (14500 kNm) in this project. In the field, the operators try to maximize the TBM penetration up to a point at which the total thrust and/or torque reach a maximum allowable value. This value is usually defined by the TBM project managers to prevent any damage to

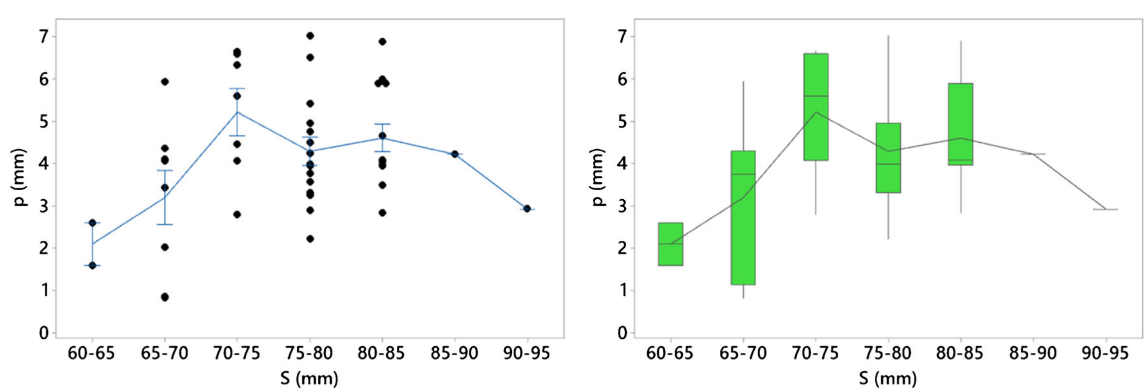

Fig. 4. Correlation between cutter spacing and cutter penetration for granitic rocks

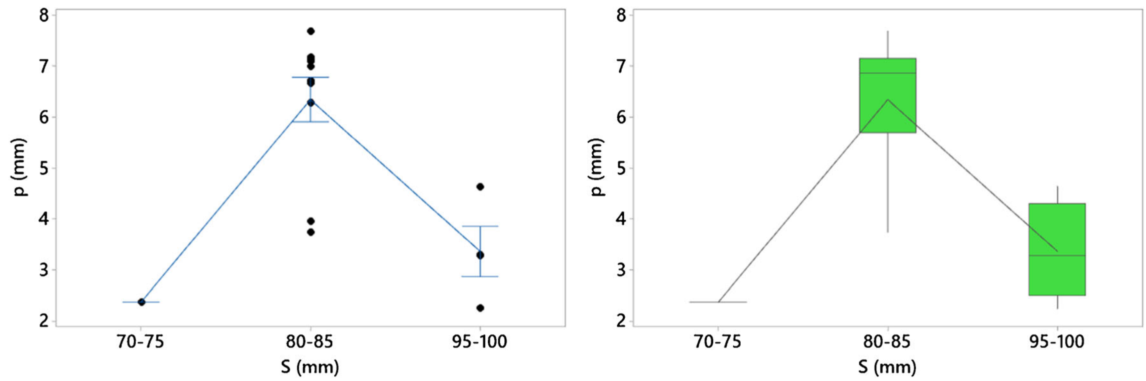

Fig. 5. Correlation between cutter spacing and cutter penetration for volcanic rocks

Table 1. Optimum cutter spacing in various rock types

Rock type	Range of cutter penetration in its *Q3* and *Q4* (mm)	Cutter spacing range (mm)	Range of cutter penetration in its *Q4* (mm)	Cutter spacing range (mm)
Sedimentary rocks	6.54–13.9	70–95	7.8–13.9	72–91
Metamorphic rocks	4.75–8.84	71–86	5.84–8.84	71–86
Granitic rocks	4.1–5.4	67–90	5.4–7	70–84
Volcanic rocks	6.3–7.7	81–85	7.1–7.7	81–85

the main bearing of the cutterhead. One major shortcoming of the laboratory tests is that the number of cuts is limited and it is not possible to observe the actual behavior of the cutters when the over-break or under-break phenomena happen. In reality, the TBM cutterhead cut the tunnel surface several hundred times at a specific set of spacing and penetration. In this case, when a rock bridge is generated and the groove is deepened, the cutter flanks will ultimately force the bridge to break. This will not happen in a couple of cutting actions. One of the major problems in numerical simulations is that the surface of the rock is not preconditioned (a process in large-scale testing to create a rough surface before conducting the main test), and this affects the final results.

In addition to these explanations, specific energy issue seems to create only one part of the puzzle of the TBM performance optimization, and other major design issues are needed to be taken into account (e.g., cutter spacing and the specification of the cutterhead layout design in various ground conditions). In this regard, field data analysis is the best way to enhance such optimization as it relies on the actual data and it covers various conditions that might not be easy to be simulated in the laboratory or by numerical modeling.

In this paper, first, an explanation is presented for the database compiled by the author during the past 10 years to investigate the parameters maximizing the field TBM penetration and advance rate. Second, the correlations between cutter penetration, cutter spacing, uniaxial compressive strength, and rock type are studied to find the range of optimum cutter spacing maximizing TBM penetration. Last, a study is conducted on the designs of the TBMs with a relatively high advance rate to identify suitable layout designs utilized in

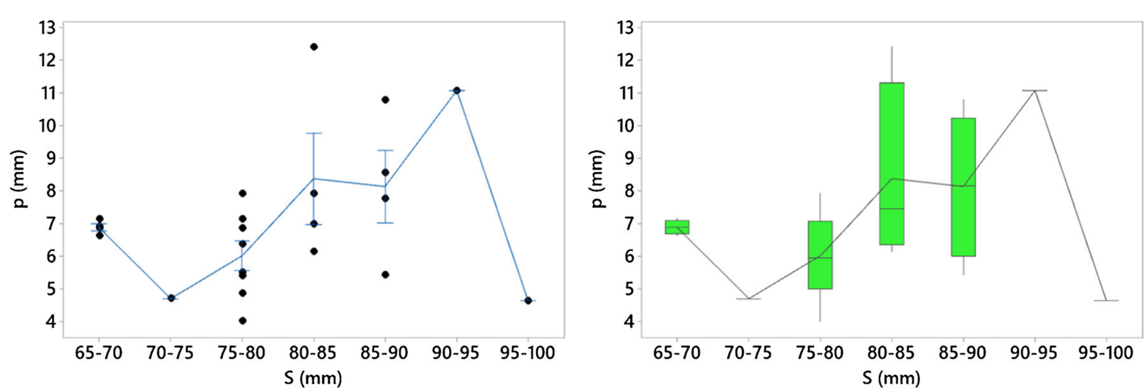

Fig. 6. Correlation between cutter spacing and cutter penetration for *UCS* below 50 MPa

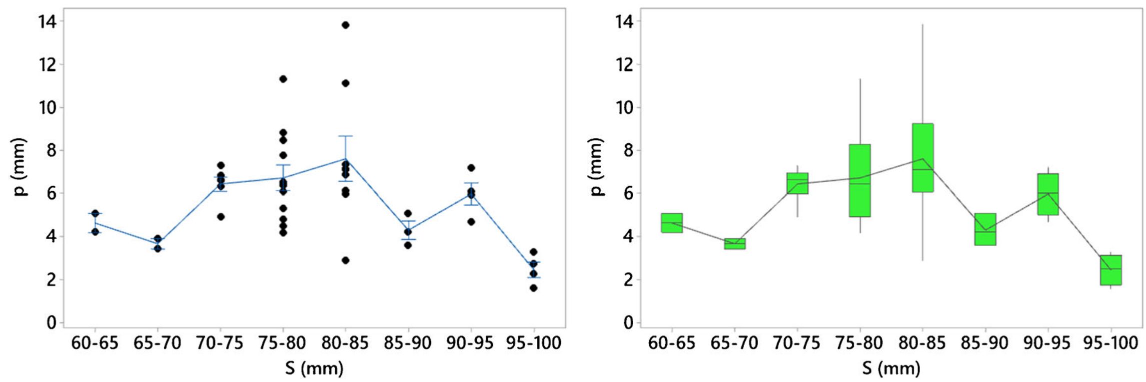

Fig. 7. Correlation between cutter spacing and cutter penetration for *UCS* between 50 and 100 MPa

various rock types. The new findings provided in this study will help the industry to enhance the specifications of hard-rock TBMs during the design phase of a project with a major goal to increase its performance during the phase of operation.

Description of the TBM field performance databases

A field performance database of hard-rock TBM projects has been compiled by gathering information from different sources. This database was set up to include the information of cut and cutter geometry information and to include their influential parameters (e.g., *UCS* and quartz content) within a geological zone of a tunnel drive. It consists of more than 300 tunnel projects. This database contains TBM diameters ranging from 1.63 to 11.52 m. TBM projects compiled in the database were completed between 1980 and 2015 with a total length of around 1500 km by three types of hard-rock TBMs (open, single-shield, and double-shield) manufactured by 8 different companies. Fig. 1 shows the distribution of the main parameters included in this database. As seen, the range of these parameters shows the database cover the majority of the values that occur in TBM tunneling projects. It is also evident from the distribution curves that the majority of the data are symmetric around the mid-point, meaning that the database information is not skewed towards a certain range of parameters. The boxplots show excavated diameter, *UCS*, cutter spacing, and cutter penetration have a range of 1.63–11.52 m, 5–350 MPa, 57–105 mm, and 0.8–17.7 mm; an interquartile range of 3.5–5.55 m, 55–140 MPa, 73–83 mm, and 4–7.1 mm; and a median of 4.12 m, 103 MPa, 78.5 mm, and 5.5 mm, respectively.

Also, the distribution curves and box plots of total thrust (*Th*), cutterhead revolution per minute (*RPM*), power (*P*), and calendar monthly advance rate (*MARc*) show they have a range of 1176–20374 kN, 0.6–16.75, 175–3150 kW, and 90–1619 m/month; an interquartile range of 5475–8872 kN, 6–11.5, 596–1200 kW, and 265–587 m/month; and a median of 7120 kN, 9.65, 783 kW, 380 m/month, respectively.

One note to consider is that there are many missing data (parameters) for various tunnel records in the database, which make it heterogeneous. This means that only a limited number of records can be used when considering a certain combination of input parameters, thus reducing the population size used in the statistical analyses. In order to reduce the uncertainty in the database values, the data is cross-checked from multiple sources of information.

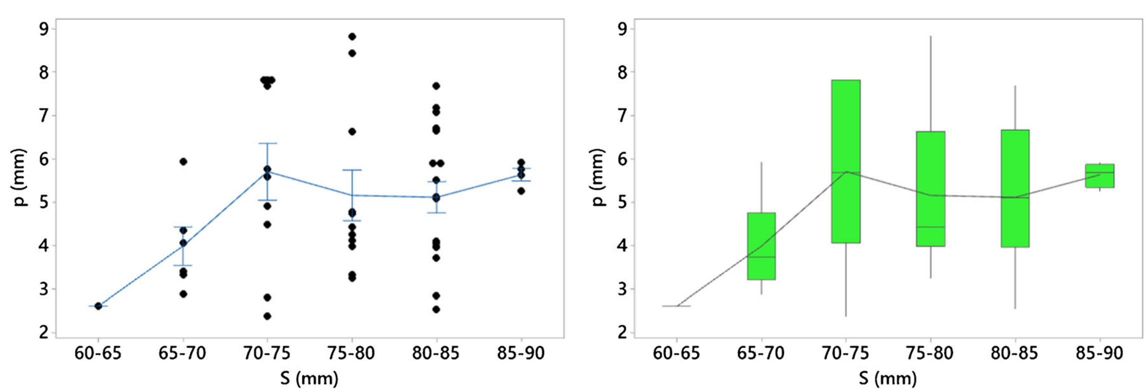

Fig. 8. Correlation between cutter spacing and cutter penetration for *UCS* between 100 and 150 MPa

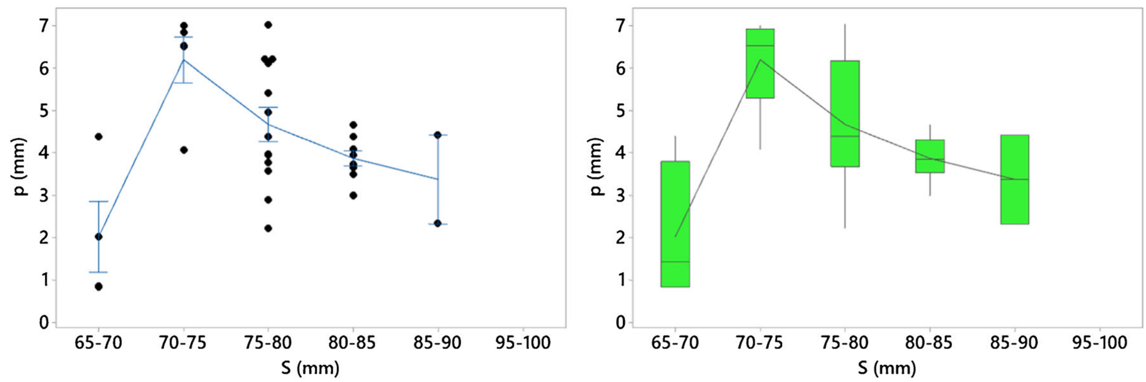

Fig. 9. Correlation between cutter spacing and cutter penetration for *UCS* over 150 MPa

Data analysis using the database

Optimum cutter spacing

In order to find the optimum cutter spacing, its variation across its influential factors is studied to find the maximum field cutter penetration. In the following sections, three major influential factors of rock type, uniaxial compressive strength (*UCS*), and quartz content (*Qtz*) are studied. In addition, the common range of values for spacing over penetration (*S/p*) are studied for the range of maximum penetrations in various rock types, quartz contents, and different categories of *UCS*. It is important to note that the size of cutters in this analysis is 17 inches.

Cutter spacing and rock type

Figs. 2–5 show the correlation between cutter spacing and penetration for four major categories of rock types, including the following:

- Sedimentary rocks (e.g., mudstone, shale, siltstone, sandstone, limestone, dolomite)
- Metamorphic rocks (e.g., marble, schist, phyllite, slate)
- Granitic rocks (e.g., granite, granodiorite, gneiss)
- Volcanic rocks (e.g., basalt, tuff)

As seen, in all figures, penetration across different spacing categories generally tends to increase, and then the trend direction reverses. It is also seen that the maximum value of the penetration in various categories of rock types coincides with different cutter spacing values. Considering the optimum cutter performance at its maximum penetration, the corresponding cutter spacing values can be identified as the optimum cutter spacing in various categories of rock types as shown in Table 1. In this table, *Q3* and *Q4* refer to the third and fourth quartiles. If we use the fourth quartile of the cutter penetration to recognize the optimum cutter spacing, it is seen that in sedimentary rocks which are usually softer, the optimum spacing can be raised to 90 mm, whereas in granitic rocks, the optimum spacing is below 85 mm. One note is that considering the rock type as the only parameter to identify the optimum cutter spacing, the achieved range is a bit large; hence; it is necessary to study the effect of other influential parameters to narrow this range.

Table 2. Optimum cutter spacing in various categories of *UCS* values

UCS category	Range of cutter penetration in its *Q3* and *Q4* (mm)	Cutter spacing range (mm)	Range of cutter penetration in its *Q4* (mm)	Cutter spacing range (mm)
Below 50 MPa	6.9–13.9	67–95	7.9–13.9	75–95
Between 50 and 100 MPa	6.1–12.4	71–90	7.1–12.4	71–90
Between 100 and 150 MPa	4.8–8.8	70–90	6.1–8.8	72–83
Above 150 MPa	4.1–7	68–85	6–7	71–79

Table 3. Description of various rock type and quartz content categories

Rock type	Rock type code *RT*	Quartz content range	Quartz content code *Qtz*
Sedimentary rocks	1	0–20%	1
Volcanic rocks	2	20–50%	2
Metamorphic rocks	3	50–75%	3
Granitic rocks	4	75–100%	4

Table 4. Minitab regression coefficient statistics for S_{opt} prediction

Term	Coef.	SE coef.	*T*-value	*p*-value	VIF
Constant	87.85	1.12	78.53	0.000	
UCS	−0.0239	0.0106	−2.25	0.033	1.65
RT	−1.663	0.440	−3.78	0.001	2.16
Qtz	−1.027	0.597	−1.72	0.047	1.47

Table 5. Results of the statistical measure for the evaluation of S_{opt}

Statistical measures	MAD	RMSE	RRMSR	MAE	MAPE
Training dataset	3.23	1.88	0.024	1.48	0.019
Testing dataset	4.56	4.05	0.051	3.4	0.042

Cutter spacing and *UCS*

Figs. 6–9 show the correlation between cutter spacing and penetration in four major categories of uniaxial compressive strength values, including the following:

- Below 50 MPa
- Between 50 and 100 MPa
- Between 100 and 150 MPa
- Above 150 MPa

In these figures, it is also seen that in general, penetration across different spacing categories generally tends to increase, and then the trend direction reverses. The maximum value of the penetration in various categories of *UCS* values coincides with different cutter spacing values. Considering the optimum cutter performance at its maximum penetration, the corresponding cutter spacing values can be identified as the optimum cutter spacing in various categories of *UCS* values as shown in Table 2. Similar to the previous section, if we use the fourth quartile of the cutter penetration to recognize the optimum cutter spacing, it is seen that in the category below 50 MPa which refers to softer rocks, the optimum spacing can be raised to 95 mm, whereas in harder rocks with *UCS* value above 150 MPa, the optimum spacing is below 80 mm.

Empirical models to evaluate optimum cutter spacing

In this section, the database is filtered to have the fourth quartile of the cutter penetration in various rock types and *UCS* categories. The result is considered the optimum rock cutting condition database.

In this database, tunnel diameter ranges from 2.7 to 11.74 m, *UCS* ranges from 5 to 230 MPa, cutter penetration ranges from 2 to 17.7 mm, and cutter spacing varies from 70 to 91 mm. Hence, the data covers almost the full spectrum of various cutting parameters. This is very important when an empirical formula is meant to be generalized. Table 3 shows the

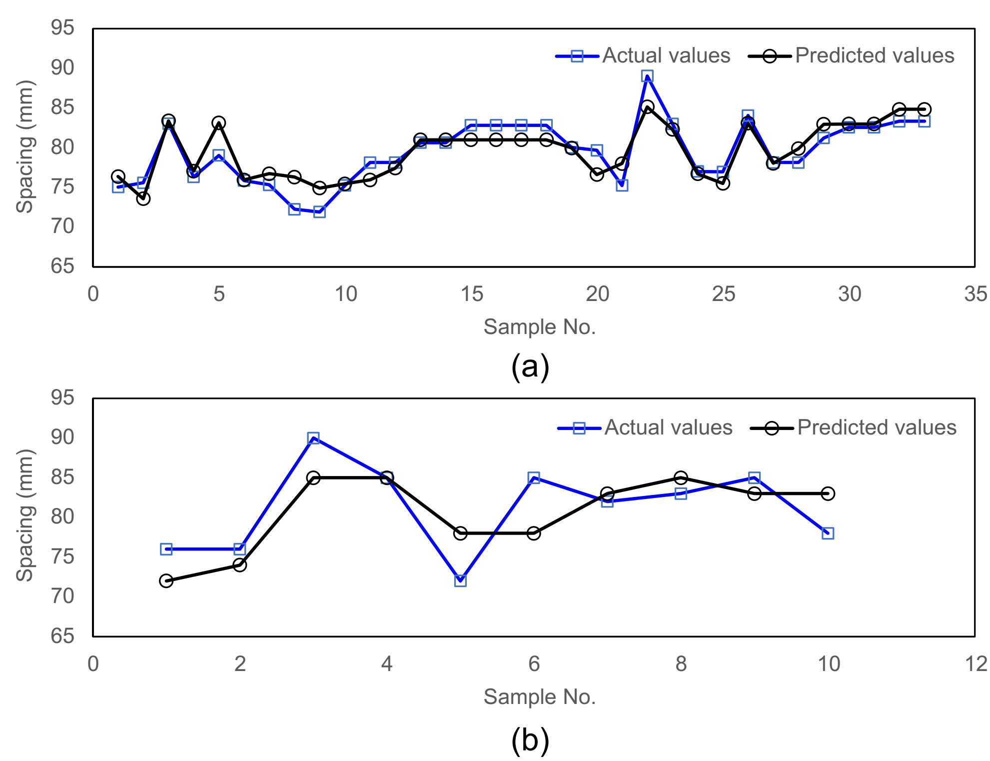

Fig. 10. The comparison between the actual and predicted values for the **a** training and **b** validation datasets

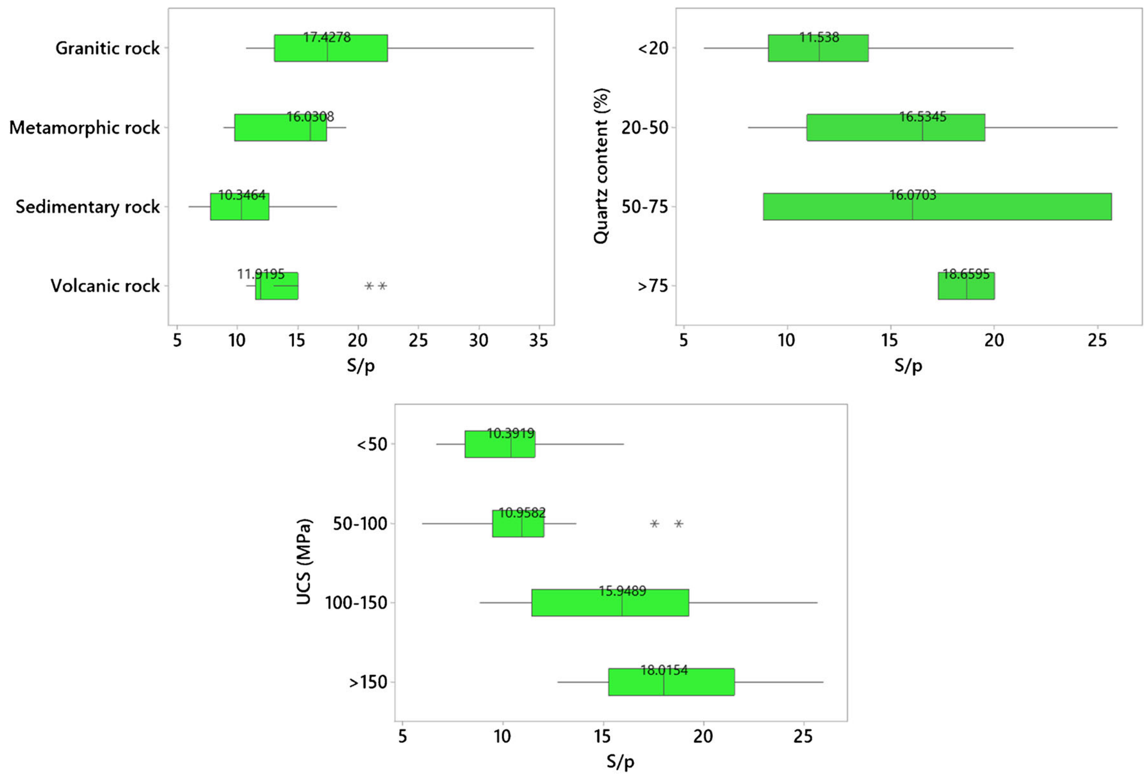

Fig. 11. Correlation between *S/p*, rock type, quartz content, and *UCS*

corresponding codes used to represent different categories of rock type and quartz content.

The correlations between optimum cutter spacing and its three major influential parameters of *UCS*, rock type code, and quartz content code show the optimum cutter spacing decreases when *UCS*, *RT*, and *Qtz* increase. The simple regression formulas are only useful when the data for more robust models (e.g., multiple regression formulas) are not available. In order to evaluate S_{opt}, with higher accuracy and to consider the combined effects of all discussed parameters, different multivariate regression analyses were run on the database information using Minitab 16. In this study, the filtered database comprises 33 samples (training dataset) which were used for the development of the statistical model, and 10 randomly selected data of TBM tunneling projects which were not used in the development of the model (validation dataset) were considered for the validation process.

The final result is presented in Eq. 1 and Table 4. As seen, the R^2 of this equation is relatively high.

$$S_{opt} = 87.85 - 0.0239\ UCS - 1.663\ RT - 1.027\ Qtz \qquad \left[R^2 = 75\%\right] \tag{1}$$

where S_{opt} is optimum cutter spacing in mm.

The comparison of the predicted versus actual cutter spacing values for both training and validation datasets is shown in Fig. 10. As seen, predicted values are in good agreement with the actual data. The obtained results were evaluated based on the statistical measures such as mean absolute deviation (MAD), root mean squared error (RMSE), relative root mean squared error (RRMSE), mean absolute error (MAE), and mean absolute percentage error (MAPE)(Table 5). The results indicate the error terms are relatively small.

Table 6. Optimum *S/p* in various categories of *UCS* values

Rock type	*S/p* interquartile range and median	Quartz content range (%)	*S/p* interquartile range and median	*UCS* category (MPa)	*S/p* interquartile range and median
Sedimentary	7.8–12.6 (10.3)	0–20	9–13.9 (11.5)	0–50	8–11.6 (10.4)
Volcanic	11.5–15 (11.9)	20–25	11–19.5 (16.5)	50–100	9.5–12 (11)
Metamorphic	9.8–17.4 (16)	25–50	9–25.7 (16.1)	100–150	11.5–19.3 (16)
Granitic	13.1–22.4 (17.4)	>75	17–20.1 (18.7)	>150	15.2–21.5 (18)

Table 7. Minitab regression coefficient statistics for $\left(\frac{S}{p}\right)_{opt}$ prediction

Term	Coef.	SE coef.	*T*-value	*p*-value	VIF
Constant	4.83	1.25	3.87	0.000	
UCS	0.040	0.0115	3.49	0.001	1.35
RT	2.486	0.463	5.37	0.000	1.35

Table 8. Results of the statistical measure for the evaluation of $\left(\frac{S}{p}\right)_{opt}$

Statistical measures	MAD	RMSE	RRMSR	MAE	MAPE
Training dataset	4.72	3.97	0.406	3.90	0.291
Testing dataset	5.18	1.54	0.132	1.27	0.103

S/p and rock type

In the literature, the optimal spacing over penetration (*S/p*) is referred to as the combination of spacing and penetration at which the energy consumption becomes lower. This is usually defined based on the results of large-scale laboratory tests (i.e., linear cutting machine or rotary cutting machine tests). Based on these tests, the optimal ratio of spacing to penetration (*S/p*) generally varies between 10 and 20 for different rocks (Ozdemir et al. 1978; Rostami 1993; Gertsch et al. 2007; Farrokh et al. 2015). In soft rocks with brittle behavior; this is closer to 10, whereas, for hard rocks with brittle behavior, this ratio is closer to 20–25 (as noted by Farrokh et al. (2015) for a granitic rock). As rock becomes more ductile, chip formation at larger spacing becomes more difficult. Hence, lower ratios of *S/p* are more appropriate for ductile rocks. As an example, Bilgin et al. (2016) showed a range of *S/p*=10–15 would lead to optimum specific excavation energy in siltstone.

As noted before, specific energy is not a major concern as the rolling force (which is the major component of the specific energy) is commonly low (majorly less than 20% of the normal force as noted by Pan et al. (2018a, 2018b, 2019), Thyagarajan (2018), Tumac and Balci (2015), Abu Bakar et al. (2014), Gertsch et al. (2007), Cho et al. (2010), Balci (2009), and Rostami (1993)) and the performance of the TBMs are not usually limited by the rolling force. In practice, the optimal set of *S* and *p* refers to a situation in which the production of the larger chips is higher (e.g., portion of chips with the size of over 2 cm as noted by Farrokh and Rostami (2007)). This can be translated into a situation in which the cutters perform at their maximum penetration for a long period. For this, in order to identify the optimum *S/p* values, we need to filter the database utilized in the previous section on the basis of the maximum achieved penetration values. In this paper, the database is filtered according to the limits of the fourth quartile of the cutter penetration achieved in various categories of the influential parameters (i.e., *UCS*, rock type, and quartz content). Fig. 11 shows the variation of *S/p* across various categories of rock type, quartz content, and *UCS*.

Table 6 summarizes the descriptive statistics of *S/p* in various categories of the noted parameters. As seen, the optimum

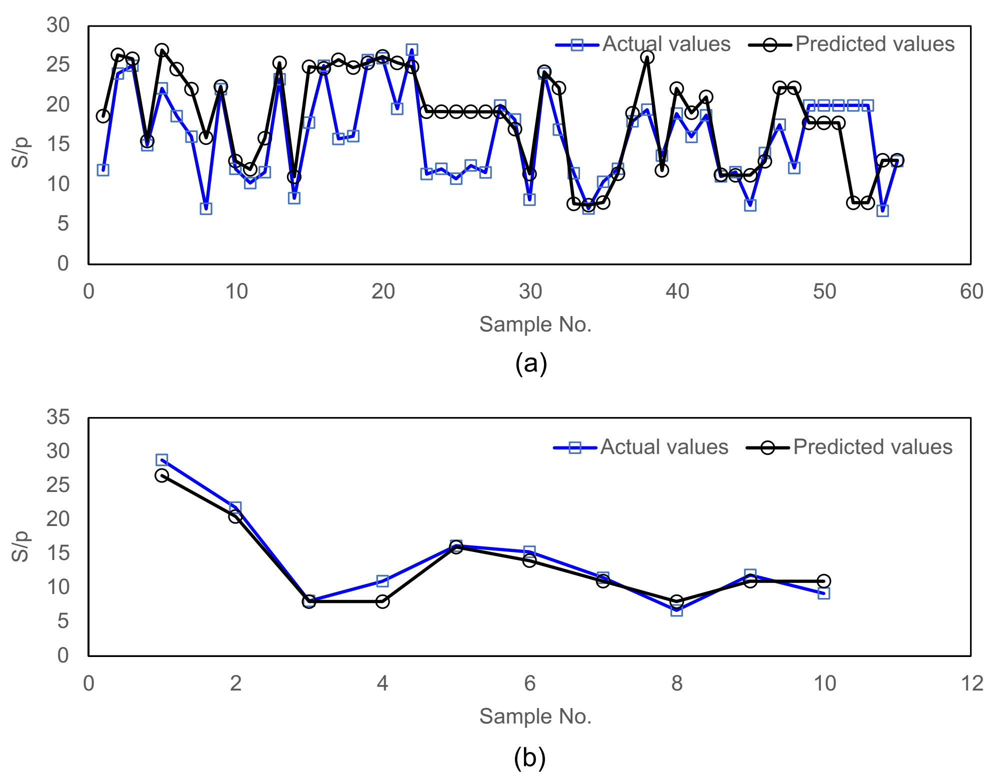

Fig. 12. The comparison between the actual and predicted values for the **a** training and **b** testing datasets

S/p tends to be lower in softer rocks with lower *UCS* values and lower quartz content (between 8 and 11.6), while in harder rocks with higher *UCS* values and higher quartz content, *S/p* is typically over 15 (between 15 and 26). This is consistent with the results of previous studies (Farrokh et al. 2015; Ozdemir et al. 1978). One note is that in designing optimum spacing and penetration, optimum spacing should be selected first (e.g., by using the optimum ranges discussed in the previous sections). This is because in evaluating the maximum cutter penetration at maximum cutter load capacity, the cutter spacing should be known first. The maximum possible penetration can be evaluated according to the cutterhead operational constraints (e.g., using the Colorado school of mines (CSM) model (Rostami 1997)). When the pair of *S* and *p* are achieved, the ratio of *S/p* is calculated and is checked to evaluate whether it is within its optimum range. If it falls outside its optimum range, it is necessary to adjust the cutter spacing and repeat this process to reach an optimum *S/p* ratio.

Empirical models to evaluate $(S/p)_{opt}$

Using the optimum rock cutting condition database (filtered database) described in the "Empirical models to evaluate optimum cutter spacing" section, the correlations among major identified influential factors and optimum ratio of cutter spacing over cutter penetration $(S/p)_{opt}$ are investigated.

Table 9. Categorization of the general layout design with respect to rock type

Layout	Rock type	Opening arrangement	Example	Comments
Radial	Flysch, Molasse	Extended close to the cutterhead center (with a length of 60 to 90% of the cutterhead radius from the cutterhead perimeter)	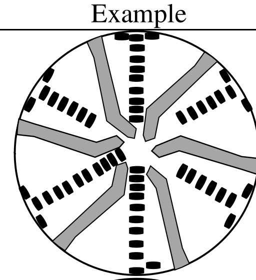	-
Complex radial	Marl, siltstone, sandstone, molasse	Extended close to the cutterhead center (with a length of up to 60 % of the cutterhead radius from the cutterhead perimeter)	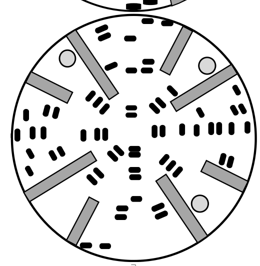	-
Evenly distributed	Majorly this layout has been used for granite and gneiss; however, it has been also used with great success for limestone, shale, and tuff	Extended to the cutterhead center with a length of up to 40 % of the cutterhead radius from the cutterhead perimeter.	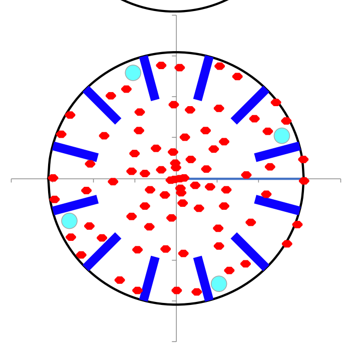	Great MARc up to 1100 m for limestone and tuff.
Double spiral	In limestone, marl, and gneiss	Extended to the cutterhead center with a length of up to 50 % of the cutterhead radius from the cutterhead perimeter.	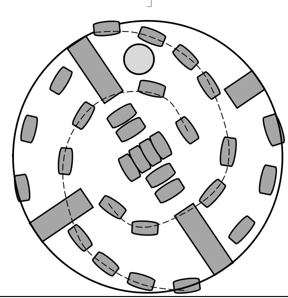	Has been used more for TBMs of around 4.5 m diameter.

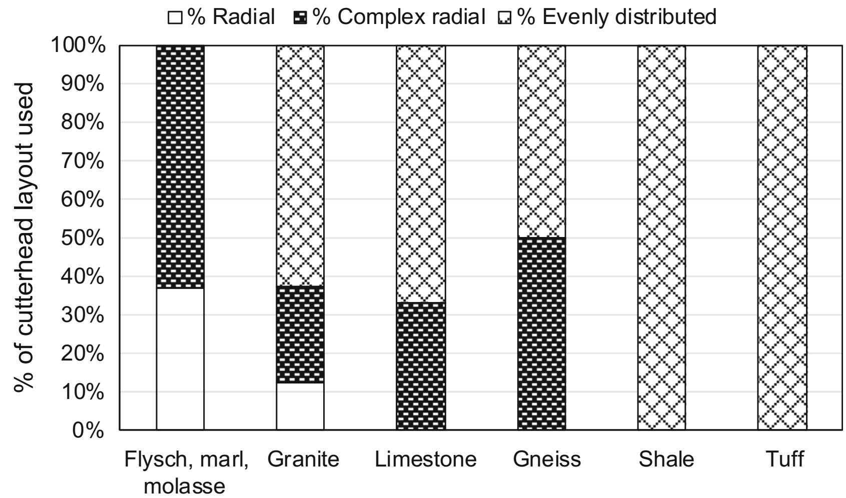

Fig. 13. Distribution of the general layout design with respect to rock type

The correlations between $(S/p)_{opt}$ and its three major influential parameters of *UCS*, rock type, and quartz content show $(S/p)_{opt}$ increases when *UCS*, *RT*, and *Qtz* increase. In order to evaluate $(S/p)_{opt}$, with a higher accuracy, different multivariate regression analyses were run on the database information using Minitab 16. The final result is presented in Eq. 2 and Table 7. In this study, the filtered database comprises 55 samples (training dataset) which were used for the development of the statistical model, and 10 randomly selected data of TBM tunneling projects which were not used in the development of the model (validation dataset) were considered for the validation process.

$$\left(\frac{S}{p}\right)_{opt} = 4.83 + 0.04\ UCS + 2.486\ RT \qquad \left[R^2 = 70\%\right] \quad (2)$$

Based on this analysis, among the input variables, *Qtz* was not statistically significant to the model (*p*-value>0.05) and was removed from the final formula.

The comparison of the predicted versus actual $\left(\frac{S}{p}\right)$ values for both training and validation datasets is shown in Fig. 12. As seen, predicted values are in good agreement with the actual data.

The performance of the developed model is also assessed in terms of the values of various statistical measures (Table 8). The results indicate the error terms are relatively small showing a close relationship between the measured and predicted values.

Layout design study

In order to study the layout design of the TBMs with good *MARc* values, there was a need to set up a criterion to filter the

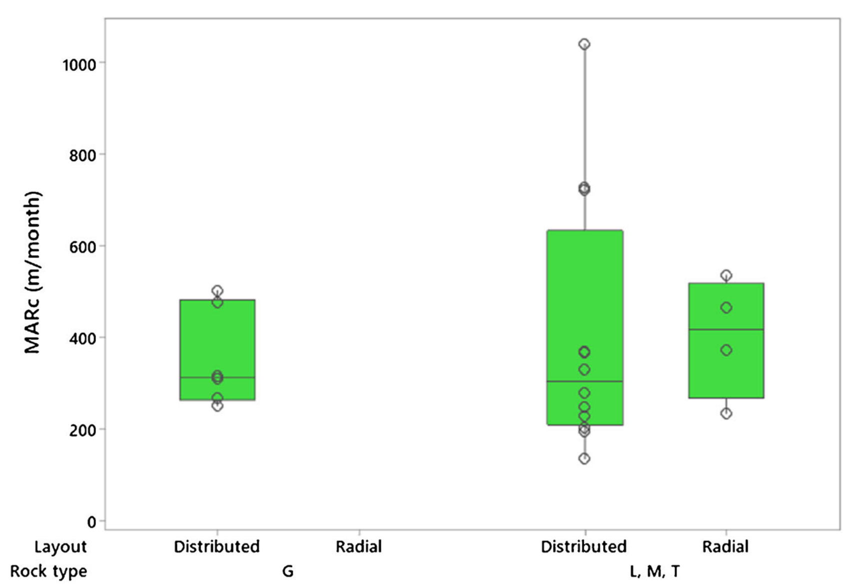

Fig. 14. The advance rate for TBMs of 8–12-m diameter in different geological conditions and with different cutterhead layouts (distributed for evenly distributed and complex radial; *G* for granite and gneiss; *L*, *M*, and *T* for limestone, marl, and tuff)

Table 10. Categorization of the general cutterhead opening design with respect to rock type and TBM diameter

TBM diameter (m)	Number of buckets	Rock type	Max bucket extension with respect to cutterhead radius	Example
<3	3-4	Limestone	35%	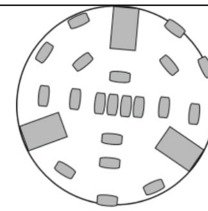
		Gneiss	25%	
4.5-5.5	4	Granite	25%	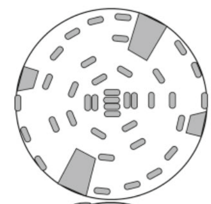
		Flysch and Marl	40-50%	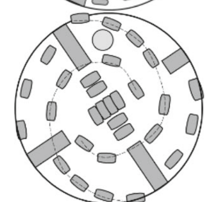
7-8.5	6	Granite and Gneiss	25-35%	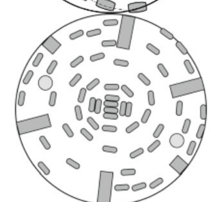
		Molasse	90%	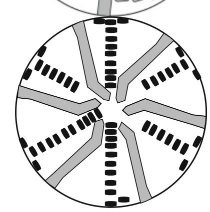
9.5-12.5	8	Limestone and Gypsum	75%	
		Granite	30%	
9.5-12.5	12	Flysch	80%	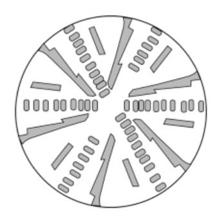
		Granite and Gneiss	20%	
12-13	16	Marl, limestone, and Molasse	60-80%	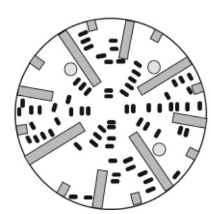
>13	>16			

database to a lower number of projects. For this purpose, the criteria of *MARc* values over its median are used. In order to account for the tunnel diameter parameter, this database is also divided into nine categories of less than 5 m, 5–10 m, and over 10-m diameter for three types of open TBM (Open), single shield TBM (SS), and double shield TBM (DS). In each category, the distribution of the *MARc* and its median is used to filter out the lower *MARc* from the higher *MARc*. With this criterion, 50 projects are filtered out to be studied as case studies with good performance. The following sections provide data analysis conducted on this reduced database.

Cutterhead layout

Table 9 and Fig. 13 show a categorization of the general layout design configurations of the cutterheads with respect to various identified rock types for the reduced database. In this table, radial layout refers to a pattern in which the cutters are located along specific radial alignments. Evenly distributed layout refers to a pattern in which the free space around the cutters is distributed more or less evenly to prevent having large free spaces in certain areas of the cutterhead (e.g., near the cutterhead periphery). The radial complex layout is a mix of two formerly explained patterns.

As seen, for flysch and molasse, because of the extension of the openings towards the center of the cutterhead, the radial and complex radial are more used due to the presence of space constraints. For granite and gneiss, the evenly distributed or complex radial patterns are more used. For tuff and shale with an RMR of over 60–70, the evenly distributed layout is used with great success.

Fig. 14 shows a comparison between the advance rates of different shielded TBMs in various rock types with a similar TBM diameter range (8–12 m). As seen, radial design is used more for flysch and molasses, while evenly distributed is used more for tuff with great success (e.g., 722 m/month for a 12.3 m double shield TBM). In the category of granite and gneiss, the evenly distributed layout is used for hard and blocky grounds with success. As a reference, in the Hallandsas tunnel project, in Granitic blocky ground, both radial and distributed layout are used, and the distributed pattern proved to be a high success in increasing cutter life (i.e., number of hours a cutter excavates before its replacement) and increasing advance rate (Burger and Dudouit 2009).

Bucket number and bucket extension

Table 10 and Fig. 15 show a categorization of major information of cutterhead openings and buckets for the projects in the reduced database.

As seen, as the TBM diameter increases, the number of buckets increases. The information also indicates that in softer rocks such as molasse, marl, and flysch, the percentage of opening extension shall be well above 50% of the cutterhead radius in order to allow a smooth flow of the excavated material from the cutterhead towards the conveyor belt. The information of this table can be used as a preliminary guideline to allocate sufficient buckets with an appropriate opening extension to maximize TBM performance.

Integrative data analysis for the layout design (Table 9) and opening design (Table 10) shows a larger opening extension limits the random distribution of the cutters. In hard and blocky grounds where the even distribution of the cutters is important, opening extension becomes shorter to allow even distribution of the cutters to crush the free blocks easier (e.g., TBMs used for Hallandsas project (Burger and Dudouit 2009) and Lotschberg project (Classen et al. 2003)). In soft and massive rocks, the even distribution of the cutters is not important as much; hence, the openings are extended towards the cutterhead center to allow higher muck volume handling from the face (e.g., TBMs used for Islisberg and Genova high-speed line tunnels (Herrenknecht web site 2021)). When the cutterhead encounters a mixed face (e.g., stratified hard and soft rocks), a complex radial layout with alternating short and long buckets is used to allow both even distribution of the cutters on the cutterhead and higher muck volume handling capacity (e.g., TBMs used for Adler, Murgenthal, and Perschling tunnels (Herrenknecht web site 2021)).

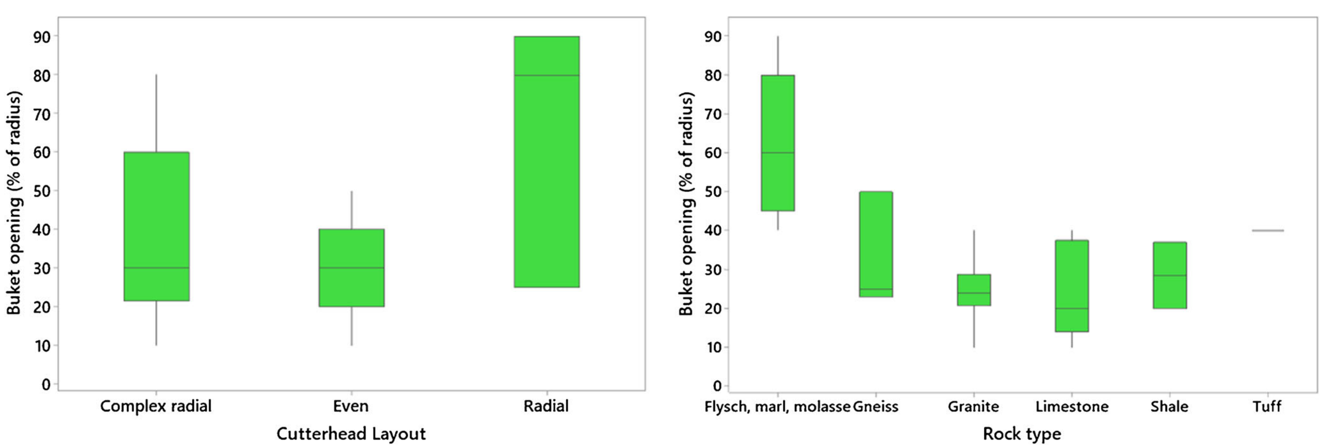

Fig. 15. Distribution of the percentage of bucket opening with respect to rock type

Number and size of the cutters and manholes

Fig. 16 shows a summary of the information of the number of gage cutters in the curved section of the cutterhead (*Ng*), number of manholes (*Nm*), number of total cutters installed on the cutterhead (*N*), number of center cutters (*Nc*), and cutter diameter (*d*) for the reduced database ("Layout design study" section). Among these parameters, the optimum number of gage cutters (*Ng*) is the most important parameter to optimize the cutting process in the curved section of the cutterhead.

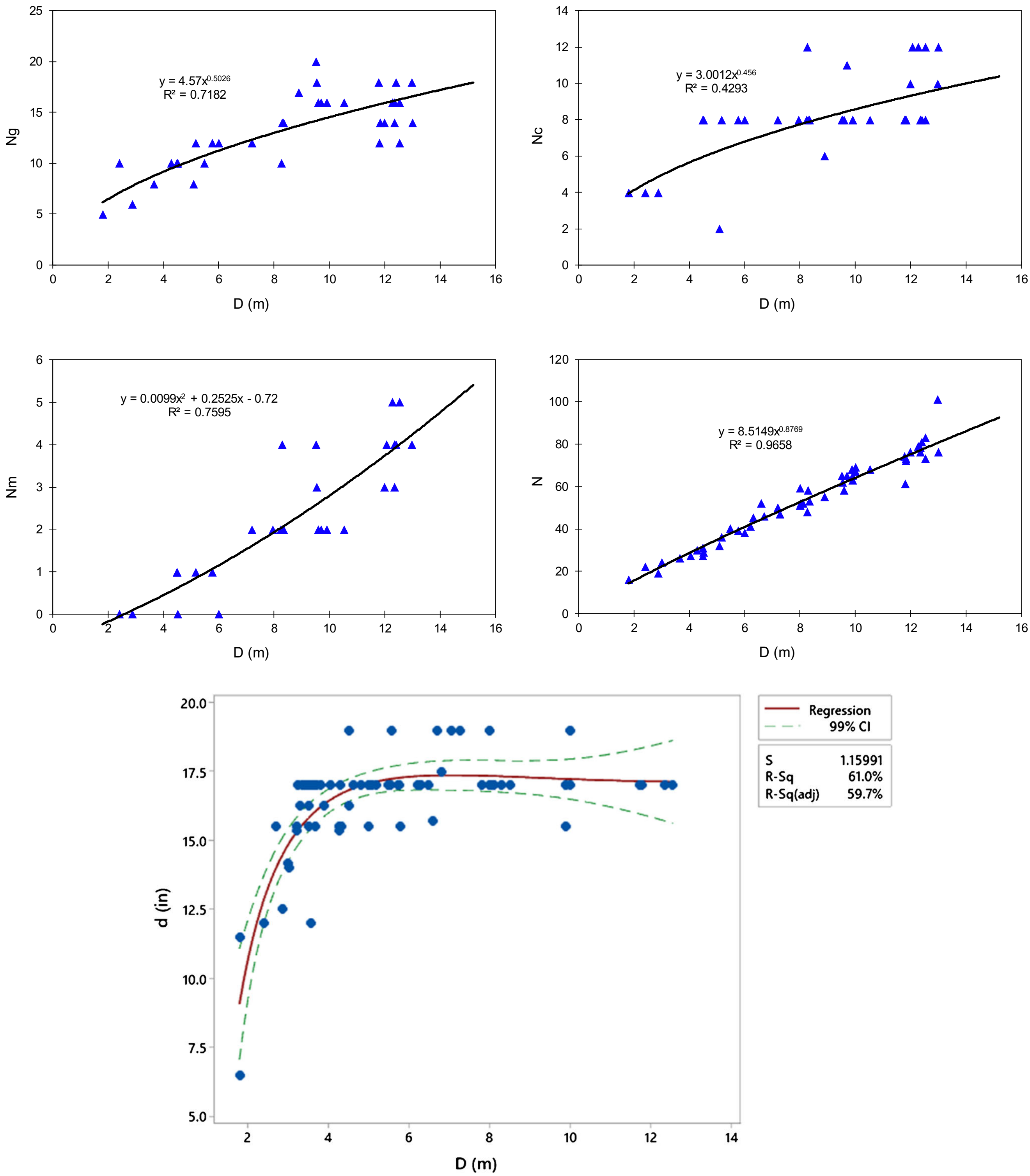

Fig. 16. Number and size of the cutters with respect to cutterhead diameter

This is because, in the peripheral area, the efficient normal force in the direction of the inclined cutters is much lower than the normal force applied to the face cutters.

TBM thrust, torque, RPM, and power

TBM design characteristics include total thrust (*Th*), cutterhead torque (*Tq*), power (*P*), and revolution per minute (*RPM*). The simple regression analyses conducted to verify the influential factors of these parameters revealed that two major parameters of the total number of cutters on the cutterhead (N_{tbm}) and cutter diameter (*d*) are highly correlated with the cutterhead design characteristics.

In the tunneling industry, empirical models are used widely due to their ease of application and due to their practical basis. In order to evaluate *Th*, *Tq*, *RPM*, and *P*, different multivariate regression analyses were run on the database information using Minitab 16. In this study, the database is randomly divided into a training dataset (with 117 samples) and a validation dataset (with 20 samples). The training dataset was used for the development of the statistical models, and the validation dataset was considered for the validation process. Eqs. 3–6 and Table 11 show the Minitab outputs for the best-fitted models for the evaluation of these design parameters based on different step forward regression analyses. It should be noted that the criterion of *p*-value less than 0.05 is used to mark the high significance of a parameter in multiple regression analysis and to include it in the final formula.

$$Th = 1.618\, N_{tbm}{}^{0.8373}\, d^{1.963} \qquad [R^2 = 81\%] \qquad (3)$$

$$Tq = N_{tbm}{}^{2.1596}\, d^{2.252}/1067 \qquad [R^2 = 85\%] \qquad (4)$$

$$RPM = 5.59\, d^{1.393}/N_{tbm}{}^{0.9838} \qquad [R^2 = 77\%] \qquad (5)$$

$$P = N_{tbm}{}^{1.1791}\, d^{3.146}/438 \qquad [R2 = 74\%] \qquad (6)$$

where *Th* is the total thrust in kN, *Tq* is the cutterhead torque in kN-m, *P* is the cutterhead power in kW, *RPM* is the cutterhead revolution per minute, N_{tbm} is the number of cutters installed on the cutterhead, and *d* is the cutter diameter in inch.

As seen, the coefficients of determination of these formulas are relatively high, making them suitable for a preliminary evaluation of the TBM design characteristics. In these formulas, when Ntbm increases, the total normal force and rolling force capacities of the cutterhead become higher; hence, the installed thrust and torque also become higher. On the other hand, in higher Ntbm, in order to limit the maximum linear speed of the gage cutters, the installed *RPM* is lowered. For all three parameters of *Th*, *Tq*, and *RPM*, when *d* increases, these parameters become higher. This is because, for larger cutters, the load and linear speed capacities are higher which allows the TBM to apply higher *Th*, *Tq*, and *RPM*.

The comparison of the predicted versus actual values for both training and validation datasets is shown in Fig. 17. As seen, predicted values are in good agreement with the actual data.

The performance of the developed models is also assessed in terms of the values of various statistical measures (Table 12). The results indicate the error terms are relatively small showing a close relationship between the measured and predicted values.

Discussion

On the basis of the discussed issues in the previous sections for the general hard-rock TBMs' cutterhead layout design specifications, in order to optimize cutter penetration and TBM cutterhead overall performance, one can utilize the following steps:

1. Calculation of the range of S_{opt} with respect to rock type, quartz content, and *UCS*
2. Calculation of S_{opt}/p range with respect to rock type, quartz content, and *UCS*
3. Calculation of the range of $(S/p)_{opt}$ using the specified cutter penetration for the project
4. Selection of specific S_{opt} range for which (S_{opt}/p) overlaps with $(S/p)_{opt}$
5. Selection of the optimum cutterhead layout with respect to rock type
6. Selection of the optimum bucket number and bucket extension with respect to TBM diameter and rock type
7. Selection of the optimum number of gage cutters, center cutters, and manholes according to the tunnel diameter

Table 11. Minitab regression coefficient statistics for *Th*, *Tq*, *RPM*, and *P* prediction

	Term	Coef	SE coef	*T*-value	*p*-value	VIF
Th	Constant	0.481	0.465	1.03	0.030	
	Ln(N_{tbm})	0.8373	0.0536	15.63	0.000	1.12
	Ln(d)	1.963	0.176	11.14	0.000	1.12
Tq	Constant	−6.973	0.818	−8.53	0.000	
	Ln(N_{tbm})	2.1596	0.0969	22.29	0.000	1.07
	Ln(d)	2.252	0.301	7.49	0.000	1.07
RPM	Constant	1.721	0.405	4.25	0.000	
	Ln(N_{tbm})	−0.9838	0.0454	−21.65	0.000	1.06
	Ln(d)	1.393	0.148	9.44	0.000	1.06
P	Constant	−6.083	0.745	−8.16	0.000	
	Ln(N_{tbm})	1.1791	0.0858	13.74	0.000	1.05
	Ln(d)	3.146	0.270	11.64	0.000	1.05

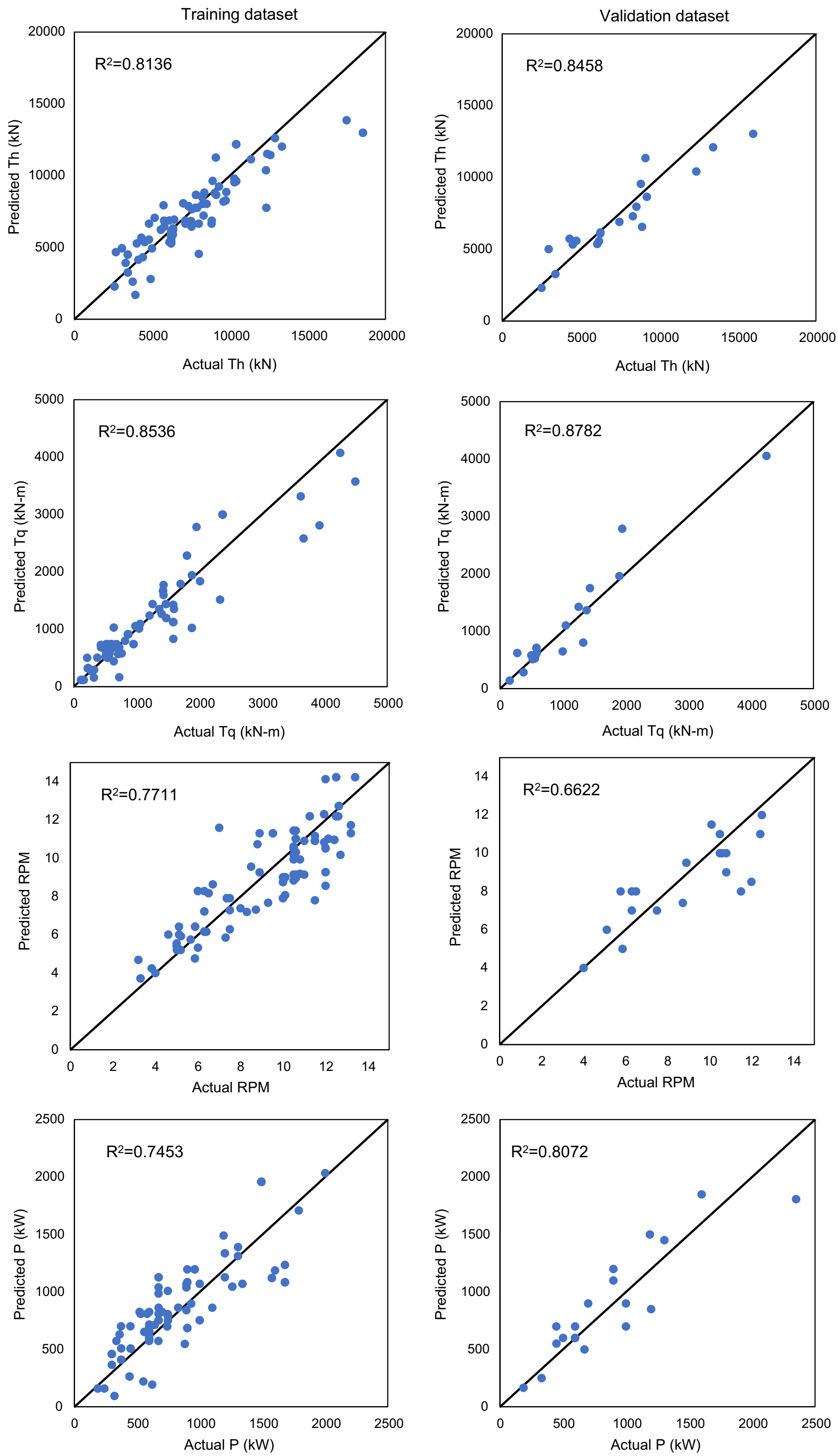

Fig. 17. The comparison between the actual and predicted values for the **a** training and **b** validation datasets

Table 12. Results of the statistical measure for the evaluation of TBM thrust, torque, RPM, and power

	Statistical measures	MAD	RMSE	RRMSR	MAE	MAPE
Th	Training dataset	2224	1402	0.205	1003	0.146
	Testing dataset	2757	1345	0.214	1072	0.156
Tq	Training dataset	694	346	0.276	228	0.203
	Testing dataset	853	462	0.300	248	0.202
RPM	Training dataset	2.45	1.33	0.158	1.04	0.120
	Testing dataset	2.34	1.55	0.176	1.24	0.144
P	Training dataset	356	264	0.327	209	0.263
	Testing dataset	505	342	0.253	234	0.221

8. Calculation of TBM thrust, torque, *RPM*, and power

As stated before, in the previous studies, the major goal in the optimization process of TBM performance is set up to reach a specific value of $(S/p)_{opt}$ at which the specific energy is at its minimum value. Minimum specific energy occurs at the minimum rolling force. The experience of applying various rolling force values at various sites shows rolling force variation usually does not change the energy consumption a lot; hence, a complementary criterion is needed to optimize the TBM performance. In practice, maximizing cutter penetration even at a cost of slightly higher energy consumption than the optimum specific energy is acceptable. The criteria, outlined in this paper, have one major goal to firstly evaluate the optimum cutter spacing based on the highest cutter penetration experienced in the field. This can be further enhanced using the new criteria to evaluate $(S/p)_{opt}$. In addition, it is tried to complement the traditional optimization process with cutterhead layout design characteristics. These are the missing links in the chain of the optimization which were neglected or at least were not discussed deeply in the previous studies. In brief, the current study tries to transfer this major idea that, optimization of *S/p*, is not enough to optimize the performance, and other design characteristics should be also considered. It is obvious that enhancing proposed strategies need further study in the future, and the author hopes to make a good first contribution in this area.

Conclusions

In this study, with the use of a compiled database of various information on many projects from around the world, an extensive data analysis is conducted to provide optimized information for hard-rock TBMs' design and performance. Considering a cross-correlation between spacing and penetration in various categories of rock types and uniaxial compressive strength values, the range of optimum cutter spacing maximizing the cutter penetration is identified. Based on the data analyses mentioned, it is found that the maximum cutter penetration in sedimentary, metamorphic, granitic, and volcanic rocks is achieved in the cutter spacing range of 72–91, 71–86, 70–84, and 81–85 mm, respectively. It is also found that the maximum cutter penetration in *UCS* values below 50, between 50 and 100, between 100 and 150, and above 150 MPa is achieved in the cutter spacing range of 72–91, 71–86, 70–84, and 81–85 mm, respectively.

Once the optimum spacing is selected, the cutterhead design parameters can be evaluated using the provided formulas. As part of the optimization of TBM cutterhead design and performance, the layout design characteristics of TBMs relatively high advance rate are studied in detail. The results show that the radial design is used more for flysch and molasses, while evenly distributed or complex radial patterns are used more for granite and gneiss with great success. For tuff and shale with an RMR of over 60–70, the evenly distributed layout can also be used with a relatively high monthly advance rate (over 400–500 m/month). The data analyses also indicate that in softer rocks such as molasse, marl, and flysch, the percentage of opening extension shall be well above 50% of the cutterhead radius to allow a smooth flow of the excavated material and to increase the TBM advance rate.

In sum, on the basis of an extensive field data and TBM cutterhead design study, using developed tables and formulas, this paper provides a basic guideline for the tunnel industry engineers to select optimum cutter spacing, optimum *S/p* ratio, number of required buckets, percentage of opening extension, and appropriate layout design characteristics, in order to maximize TBM performance parameters, including cutter penetration and TBM advance rate. The new findings offer a new horizon for the researchers to initiate various types of cutterhead optimization in addition to specific energy in the upcoming field projects and future studies.

Declarations

Conflict of interest The authors declare that they have no competing interests.

References

Abu Bakar MZ, Gertsch L, Rostami J (2014) Evaluation of fragments from disc cutting of dry and saturated sandstone. Rock Mech Rock Eng 47(5):1891–1903

Balci C (2009) Correlation of rock cutting tests with field performance of a TBM in a highly fractured rock formation: a case study in Kozyatagi-Kadikoy metro tunnel, Turkey. Tunn Undergr Space Technol 24(4):423–435

Bilgin N, Copur H, Balci C (2016) TBM excavation in difficult ground condition. Ernst & Sohn, Germany

Burger W, Dudouit F (2009) The Hallandsås dual mode TBM. Rapid Excavation and Tunneling Conference, Las Vegas, USA.

Cho JW, Jeon S, Yu SH, Chang SH (2010) Optimum spacing of TBM disc cutters: a numerical simulation using the three–dimensional dynamic fracturing method. Tunn Undergr Space Technol 25(3): 230–244

Cho JW, Jeon S, Jeong HY, Chang SH (2013) Evaluation of cutting efficiency during TBM disc cutter excavation within a Korean granitic rock using linear-cutting-machine testing and photogrammetric measurement. Tunn Undergr Space Technol 35:37–54

Choi SW, Chang SH, Park YT, Lee GP, Bae GJ (2014) Comparative analysis of cutter acting forces and axial stresses of single and double-disc cutters by linear cutting tests. J Korean Tunn Undergr Space Assoc 16(2):181–191

Classen J, Holter KG, Kurth T (2003) The AlpTransit Lötschberg Project, Switzerland. High-performance wet-mix sprayed concrete during TBM excavation of two high speed railway tunnels. In: Proc Rapid Excavation and Tunneling Conference. Society of Mining Engineers, Littleton CO, USA, 1175–1190

Eskikaya S, Bilgin N, Balci C, Tuncdemir H (2005) From research to practice: development of rapid excavation technologies. In: Erdem, Solak (eds) Underground Space Use: Analysis of the Past and Lessons for the Future. Taylor & Francis Group, London, pp 435–441

Farrokh E, Rostami J (2007) The relationship between tunnel convergence and TBM operational parameters and chip size for double shield TBMs. RETC, Canada, pp 1094–1108

Farrokh E, Kim DY, Kyung SB (2015) Rotary cutting test for hard-rock TBM performance evaluation. World tunneling conference, Dubrovnik

Gertsch R, Gertsch L, Rostami J (2007) Disc cutting tests in Colorado Red Granite: implications for TBM performance prediction. Int J Rock Mech Min Sci 44(2):238–246

Gong QM, Jiao YY, Zhao J (2006a) Numerical modelling of the effects of joint spacing on rock fragmentation by TBM cutters. Tunn Undergr Space Technol 21(1):46–55

Gong QM, Zhao J, Hefny AM (2006b) Numerical simulation of rock fragmentation process induced by two TBM cutters and cutting space optimization. Tunn Undergr Space Technol 21(3–4):263

Gong QM, He GW, Zhao XB, Ma HS, Li XZ, Zhang H, Miao CT (2015) Influence of different cutter spacings on rock fragmentation efficiency of Beishan granite by TBM. Chin J Geotech Eng 37(1):54–60 in Chinese

Gong QM, Du XL, Li Z, Wang QX (2016a) Development of a mechanical rock breakage experimental platform. Tunn Undergr Space Technol 57:129–136

Gong QM, Dong GL, Yin LJ, Ma S, Lu JW (2016b) Comparison study on the rock linear and rotating cutting tests by TBM cutter. Constr Technol 46(11):61–66 (in Chinese)

Gong QM, He GW, Zhao XB, Zhang H, Miao CT, Yao XH, Li XZ (2016c) Influence of penetration on the rock-breakage efficiency of a TBM cutter. Mod Tunn Technol 53(1):62–68 in Chinese

Herrenknecht web site, 2021 https://www.herrenknecht.com, visited on 1/27/2021.

Innaurato N, Oggeri C, Oreste PP, Vinai R (2007) Experimental and numerical studies on rock breaking with TBM tools under high-stress confinement. Rock Mech Rock Eng 40(5):429–451

Labra C, Rojek J, Oñate E (2016)Discrete/finite element modelling of rock cutting with a TBM disc cutter. Rock Mech Rock Eng 50(3):621–638

Liu HY, Kou SQ, Lindqvist P, Tang CA (2002) Numerical simulation of the rock fragmentation process induced by indenters. Int J Rock Mech Min Sci 39:491–505

Liu QS, Pan YC, Liu JP, Kong XX, Shi K (2016a) Comparison and discussion on fragmentation behavior of soft rock in multi-indentation tests by a single TBM disc cutter. Tunn Undergr Space Technol 57:151–161

Liu QS, Pan YC, Kong XX, Liu JP, Shi K, Cui XZ, Huang SB (2016b) Experimental investigation on mudstone fragmentation characteristics in indentation process by TBM disc cutter. Rock Soil Mech 37(s1):166–174 (in Chinese)

Liu QS, Pan YC, Liu JP, Kong XX, Shi K, Liu Q (2016c) Analysis on fragmentation behavior of rocks in indentation tests by disc cutter. Chin J Rock Mech Eng 35(s2):3516–3525 (in Chinese)

Ma HS, Yin LJ, Ji HG (2011) Numerical study of the effect of confining stress on rock fragmentation by TBM cutters. Int J Rock Mech Min Sci 48(6):1021–1033

Ma HS, Gong QM, Wang J, Yin LJ, Zhao XB (2016a) Study on the influence of confining stress on TBM performance in granite rock by linear cutting test. Tunn Undergr Space Technol 57:145–150

Ma HS, Gong QM, Wang J, Zhao XB, Yin LJ, Miao CT, He GW (2016b) Linear cutting tests on the effect of confining stress on rock fragmentation by TBM cutter. Chin J Rock Mech Eng 35(2):346–355

Ozdemir L, Miller R, Wang FD (1978) Mechanical tunnel boring prediction and machine design. NSF APR73- 07776-A03. Colorado School of Mines, Golden, Colorado

Pan YC, Liu QS, Liu JP, Huang X, Liu Q, Peng XX (2018a) Comparison between experimental and semi–theoretical disc cutter cutting forces: implications for frame stiffness of the linear cutting machine. Arab J Geosci 11, 266.

Pan YC, Liu QS, Liu JP, Liu Q, Kong XX (2018b)Full–scale linear cutting tests in Chongqing Sandstone to study the influence of confining stress on rock cutting efficiency by TBM disc cutter. Tunn Undergr Space Technol 80:197–210

Pan YC, Liu QS, Peng XX, Liu Q, Liu JP, Huang X, Cui X, Cai T (2019)Full-scale linear cutting tests to propose some empirical formulas for TBM disc cutter performance prediction. Rock Mech Rock Eng 52:4763–4783

Park J, Kang H, Lee J, Kim J, Oh J, Cho J, Rostami J, Kim H (2018) A study on rock cutting efficiency and structural stability of a point attack pick cutter by lab-scale linear cutting machine testing and finite element analysis. Int J Rock Mech Min Sci 103:215–229

Qi G, Zhengying W, Hao M (2016) An experimental research on the rock cutting process of the gage cutters for rock tunnel boring machine (TBM). Tunn Undergr Space Technol 52:182–191

Rostami J (1993) Design optimization, performance prediction and economic analysis of tunnel boring machine for the construction of the proposed Yucca Mountain nuclear waste repository. MS Thesis, Colorado School of Mines, Golden, Colorado, USA.

Rostami J (1997) Development of a force estimation model for rock fragmentation with disc cutters through theoretical modeling and physical measurement of crushed zone pressure. PhD Thesis, Colorado School of Mines, Golden, Colorado, USA, p 249.

Roxborough FF, Phillips HR (1975) Rock excavation by disc cutter. Int J Rock Mech Min Sci Geomech Abstr 12(12):361–366

Sanio HP (1985) Prediction of the performance of disc cutters in anisotropic rock. Int J Rock Mech Min Sci 22(3):152–163

Snowdon RA, Ryley MD, Temporal J (1982) A study of disc cutting in selected British rocks. Int J Rock Mech Min Sci Geomech Abstr 19(3):107–121

Thyagarajan MV (2018) The comparison of cutting forces on disc cutters in constant vs variable penetration modes. MS thesis, Colorado School of Mines, Golden, Colorado, USA.

Tumac D, Balci C (2015) Investigations into the cutting characteristics of CCS type disc cutters and the comparison between experimental, theoretical and empirical force estimations. Tunn Undergr Space Technol 45:84–98

Tuncdemir H, Bilgin N, Copur H, Balci C (2008) Control of rock cutting efficiency by muck size. Int J Rock Mech Min Sci 45(2):278–288